Fungal Genetics and Biology 47 (2010) 522–530

Contents lists available at ScienceDirect

Fungal Genetics and Biology

journal homepage: www.elsevier.com/locate/yfgbi

Fungal network responses to grazing

Lynne Boddy [a,*], Jonathan Wood [a], Emily Redman [a], Juliet Hynes [a], Mark D. Fricker [b]

[a] Cardiff School of Biosciences, Cardiff University, Biomedical Building, Museum Avenue, Cardiff CF10 3AX, UK
[b] Department of Plant Sciences, University of Oxford, South Parks Road, Oxford, OX1 3RB, UK

ARTICLE INFO

Article history:
Received 29 September 2009
Accepted 25 January 2010
Available online 6 February 2010

Keywords:
Adaptive network
Collembola
Fungal mycelium
Fungal stem cells
Fractal behaviour
Network resilience
Phanerochaete velutina
Saprotrophic basidiomycetes

ABSTRACT

Mycelial networks operate on scales from microscopic to many m^2 and naturally persist for extended periods. As fungi exhibit highly adaptive development, it is important to test behavioural responses on natural substrata with realistic nutrient levels across a range of spatial scales and extended time periods. Here we quantified network responses over 7.5 months in large (57 × 57 cm) microcosms to test whether grazing shifts the network to a more resilient architecture. Resource limitation constrained any ability to respond at all, with both grazed and ungrazed networks gradually thinning out over time. Added resources sustained further exploratory growth, but only transiently increased cross-connectivity and network resilience, when tested by simulated damage *in silico*. Grazed networks were initially weaker and emergence of new exploratory growth was curtailed. However, increased interstitial proliferation led to new cross-links, consolidating the existing mycelial network and increasing the resilience of the network to further attack.

1. Introduction

The vast majority of higher fungi develop as a mycelial network through hyphal tip growth, hyphal branching and fusion to give a radial branching tree with a limited number of tangential interconnections (Bebber et al., 2007a; Fricker et al., 2007a, 2008a; Lamour et al., 2007; Rayner et al., 1994, 1999). As the network grows it is continuously remodelled, with hyphae regressing in some regions and, in large mycelia, aggregating to form linear organs such as cords and rhizomorphs (Boddy et al., 2009; Cairney, 2005; Fricker et al., 2007a, 2008a; Rayner et al., 1994, 1999). The mechanism of cord thickening is thought to involve aligned growth of new hyphae and limited differentiation to give larger, thin-walled vessel hyphae and tough thick-walled fibre hyphae (Moore, 1995). It is likely that cord formation is accompanied by secretion of additional extra-cellular matrix leading to greater adhesion and insulation of the cord boundary (Rayner, 1991; Rayner et al., 1994). In addition, tendril hyphae have been observed to coil around hyphae in the cord (Moore, 1995) and may assist in bundling and compaction of the cord.

The resulting networks may occupy only a few square centimetres or, in the case of ectomycorrhizal and saprotrophic cord-forming basidiomycetes, form extensive mycelial networks in soil spanning many square metres. These networks may actively forage for new resources through exploration, or await stochastic arrival of new resources or hosts (Boddy, 1993, 1999; Boddy et al., 2009; Leake et al., 2004). To function efficiently these large networks must transport nutrients between spatially separated sources and sinks, respond rapidly to encounter with new resources, combat rivals and maintain structural continuity in the face of attack by mycophagous invertebrates or random damage (Bebber et al., 2007a; Boddy and Jones, 2007, 2008; Fricker et al., 2007a; Rayner et al., 1999). This requires a flexible strategy to partition limited resources among the competing requirements. Furthermore, the range of network architecture and dynamic behaviour amongst different species suggests that different compromises provide viable solutions to balance transport capacity, combativeness, robustness to damage and construction cost (Bebber et al., 2007a; Boddy, 1993, 1999; Boddy et al., 2009; Fricker et al., 2007a).

Quantitative analysis of mycelial network structure, development, dynamics and function is in its infancy. The macroscopic behaviour of the colony can be measured by its radial growth rate, the surface area covered by the mycelium (hyphal coverage) and box-count mass fractal dimension (D_{BM}) or surface fractal dimension (D_{BS}) (Boddy and Donnelly, 2008; Boddy et al., 1999; Donnelly et al., 1995; Senesi and Boddy, 2002). At finer resolution, the network architecture can be determined directly from the cord connections, branch points and fusions (Bebber et al., 2007a,b; Boddy et al., 2009; Fricker et al., 2007a, 2008a,b; Lamour et al., 2007; Rotheray et al., 2008) using tools developed in graph theory (Albert and Barabasi, 2002; Amaral and Ottino, 2004; Dorogovtsev and Mendes, 2002; Newman, 2003).

* Corresponding author. Fax: +44 0 29 208 74116.
E-mail address: BoddyL@cardiff.ac.uk (L. Boddy).

1087-1845/$ - see front matter © 2010 Elsevier Inc. All rights reserved.
doi:10.1016/j.fgb.2010.01.006

Previous work with *Phanerochaete velutina* has shown that it forms robust networks with high transport efficiency that are resistant to damage. Furthermore, this is achieved with a relative decrease in overall cost, on a unit area basis, by reinforcement of key pathways and recycling of unwanted interstitial mycelium (Bebber et al., 2007a). Within this overall pattern, the network architecture is further modified in response to other fungi or grazing by collembola (Rotheray et al., 2008). Dynamic imaging of nutrient transport, visualised using radiolabel movement and photon-counting scintillation imaging, has shown that N-resources are preferentially allocated to C-rich sinks (Tlalka et al., 2008a), and that there is a strong pulsatile component to transport (Fricker et al., 2007b; Tlalka et al., 2007).

However, all these previous transport and network studies with *P. velutina* have been conducted in small (12×12 cm or 25×25 cm) microcosms from agar or wood block inocula that have been colonised by mycelia growing on rich media (Bebber et al., 2007a; Fricker et al., 2007b; Rotheray et al., 2008; Tlalka et al., 2007, 2008a,b). Under these conditions, the initial dense, radial symmetric growth phase tends to reflect the mycelial response to high nutrients that are sequestered by mycelium during the initial colonisation phase (Tlalka et al., 2008a). Such conditions would be encountered relatively rarely in the natural environment, which is characterised by low overall resource levels and high C:N ratio, although C:N ratio decreases considerably as decomposition proceeds (Watkinson et al., 2006). In addition, observations are typically made over limited time periods (2–6 weeks), not least because growth is constrained by the microcosm boundary. As fungi are characterised by exceptionally adaptive responses to the environment and prevailing heterogeneous nutrient regime, it is important to test fungal responses on natural substrata across a range of spatial scales with realistic nutrient levels and long time periods, particularly as the success of the foraging and survival strategy would be evaluated over at least an annual cycle *in situ* (Boddy, 1999).

Here we examine adaptive network responses under nutrient limitation and grazing pressure over an extended time period to determine how the priority of resource allocation alters under nutrient limitation (Bebber et al., 2007a), and test whether adaptation to grazing pressure shifts the network to a more resilient architecture (Rotheray et al., 2009). To this end mycelial systems of *P. velutina* were allowed to grow in large (57×57 cm) non-sterile soil-based microcosms with minimal physical constraints, before the introduction of collembola grazing pressure and additional natural wood block resources.

2. Methods

2.1. Soil microcosms

The work extends a 99 d study (Wood et al., 2006) to 208 d and full details of the experimental procedure and design have been given in Wood et al., 2006. In brief, beech (*Fagus sylvatica)* wood blocks ($2 \times 2 \times 1$ cm) precolonised by *P. velutina* were inoculated centrally onto 57×57 cm square trays of compacted non-sterile soil. After 36 d, when mycelia had a mean radial extent of 20 cm, a further four sterile beech wood blocks ($2 \times 2 \times 1$ cm) were added to 20 randomly selected trays, approx 5 cm from the edge of the tray, at the centre of each side (Fig. 1). Of these 20 trays, 10 were randomly selected and inoculated each with 250 laboratory-reared *Folsomia candida* at 49 d to give a density of $\sim$800 m^{-2}. This is less than usual field densities of around 10^4–10^5 m^{-2} (Petersen and Luxton, 1982), but still constitutes a substantial grazing pressure on the fungal mycelium in the absence of any other source of food. A further 10 trays, without the additional resources were also inoculated with 250 *F. candida* each, leaving 10 other trays with no additional resources and no collembola added, thus creating four treatments: (1) no additional resources and no collembola (R^-C^-); (2) no additional resources and 250 collembola (R^-C^+); (3) additional resources and no collembola (R^+C^-); (4) additional resources and 250 collembola (R^+C^+). Trays were incubated at 19 °C in the dark, in black polythene bags above trays of water to maintain humidity. They were monitored weekly and moistened by misting with deionised water. Each treatment initially had 10 replicates, but due to contamination by soil fungi or physical damage, only seven of each group remained by 208 d.

2.2. Image capture and analysis

Digital images of the growing systems were captured initially at 4–10 d intervals and then at longer intervals of 1–2 months, from a height of 82 cm, using a Konica Minolta Revio KD-420Z digital camera (Wood et al., 2006). Images (2272×1704 pixels) were cropped and resized using IMAGEJ (National Institute of Health, USA) to contain just the trays at a size of 1500×1500 pixels, and then converted to greyscale (8 bit) .tif file format.

To determine hyphal coverage (*HC*) and box-count mass fractal dimension (D_{BM}), wood blocks, tray edges and vacant areas of soil were edited manually from the image to leave just the mycelium. The mycelium was then segmented from the background using a manual threshold (Wood et al., 2006) and used to determine *HC* from the binarised image with appropriate calibration. D_{BM} of the whole mycelium was determined by the box-counting method (Obert et al., 1990; Senesi and Boddy, 2002), with a degree of three pixels, using the IMAGEJ plugin FracLac (Karperien, 2003). Repeated measures analysis of variance (ANOVA) was used for making comparisons between mean hyphal coverage and between D_{BM} data. Data were normally distributed (Kolmogorov–Smirnov test), had equal variance (Levenes's test) and displayed sphericity (Mauchly's test) thus satisfying assumptions of repeated measures ANOVA. The Tukey–Kramer *a posteriori* test was used to test for significant differences between means. Data are presented with standard error of the mean, unless otherwise stated. One way ANOVA was also used to make comparisons between treatments at specific time points from 99 d onwards.

2.3. Analysis of network architecture

The digital images of three randomly selected ungrazed and three grazed mycelia with added resources, at 36, 57, 78, 99, 155 and 208 d, were imported and aligned in a custom built MatLab (The MathWorks Inc., Nantick, MA) program, as described previously (Bebber et al., 2007a; Fricker et al., 2008b). The network was extracted as a series of N nodes, each representing a tip, branch or anastomosis, joined by a set of M links representing the intervening cords from a randomly selected quarter of each tray, such that a new resource was present within the networked area. Node positions were stored as a list of their Cartesian (x, y) coordinates, whilst links were stored as a weighted $N \times N$ adjacency matrix, where each entry represents the diameter of the link between node i and node j (d_{ij}). Both the inoculum and added resource were represented as single nodes since the internal mycelial connections were unknown. Cord diameters were estimated from the reflected light intensity using an experimentally determined calibration (Bebber et al., 2007a; Fricker et al., 2008b). The cost of each link was estimated from its length (l_{ij}) times the cross-sectional area ($a_{ij} = \pi(d_{ij}/2)^2$). This approximation does not take into account any variation in the internal structure of the cords due to the presence of fibre hyphae or larger, thin-walled vessel hyphae (Eamus et al., 1985; Thompson and Rayner, 1982). The link weight was colour-coded across the network according to a rainbow scale,

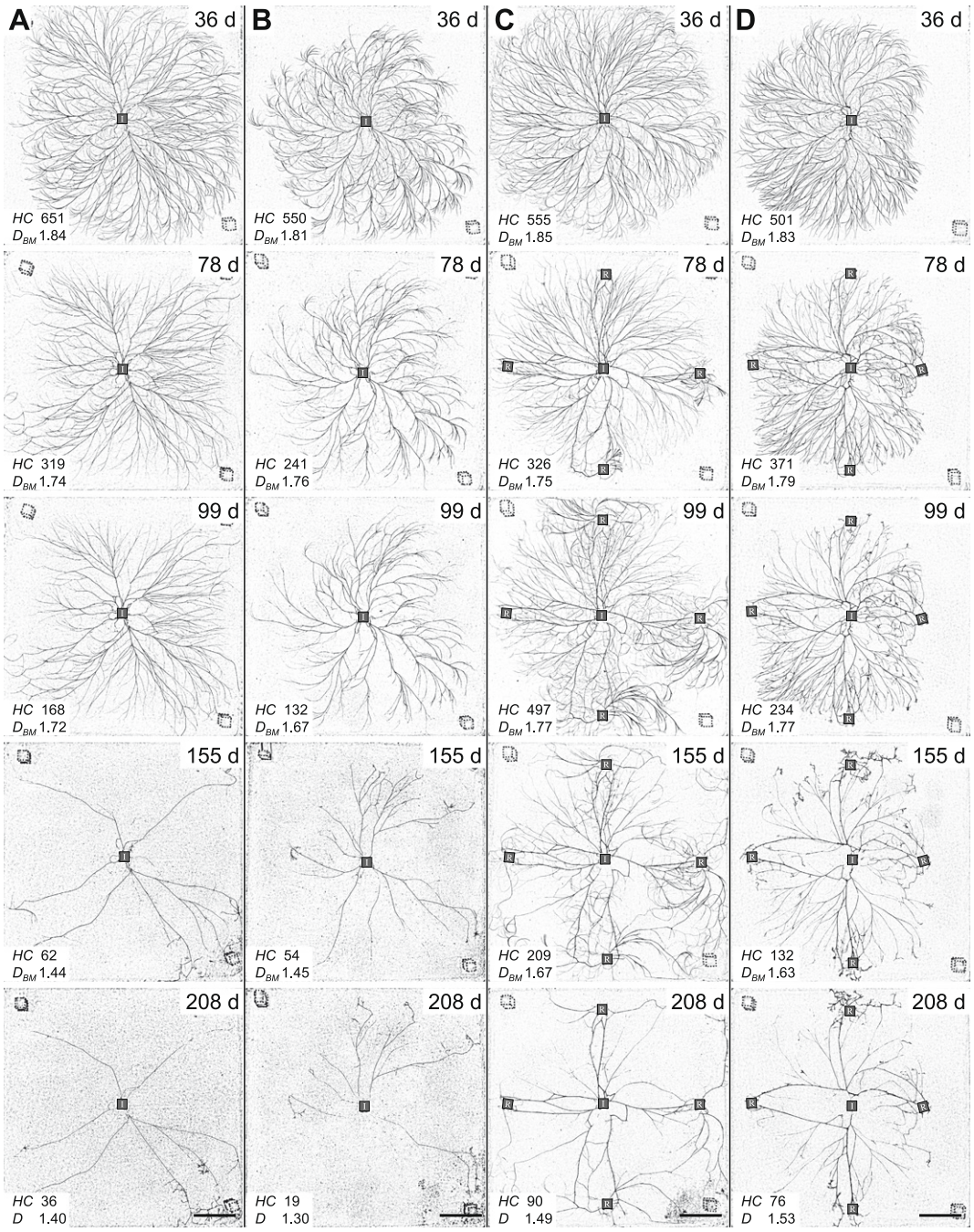

Fig. 1. The effect of added resources and grazing on the development of *Phanerochaete velutina*. Representative images of mycelial systems of *P. velutina* grown from beech wood blocks (I) in trays (57 × 57 cm) of compressed non-sterile soil are shown at the timepoints indicated for four treatments. For display, images were processed by background subtraction, contrast-limited histogram equalisation, contrast stretching and look-up table inversion to give black-on-white representations of the colony morphology. A - ungrazed with no additional resources; B - grazed (250 collembola) with no additional resources; C - ungrazed with additional resources (R); D - grazed, with additional resources. New resources and collembola, when present, were added at 36 d and 49 d, respectively. Mass fractal dimension (D_{BM}) and hyphal coverage (*HC*, cm^2) are presented bottom left of each image. The position of Perspex lid supports are indicated by dotted outlines. Scale bar = 10 cm.

with red representing thick cords. Development or regression of links was measured as the difference in cord diameter over the total interval 36–208 d ($\Delta d_{ij} = d_{ij(t=208)} - d_{ij(t=36)}$), normalised to the maximum range of the difference, $\Delta d_{ij}/(d_{ij,\max} - d_{ij,\min})$. This gives a value of 1 for consistently growing cords, a value of −1 for cords that shrink and 0 for cords that essentially remain constant over the time interval. Results for the link evolution were expressed as a rainbow scale, with red representing continuous growth.The weighted adjacency matrices, node positions and node identities were exported to R 1.9.0 (R Development Core Team, 2007) to evaluate network structure and performance (Bebber et al., 2007a; Fricker et al., 2008b). The total cost was used as a proxy for the biomass using the assumptions given above for cord structure, and was estimated from the sum of the costs for each link, $\sum_{i \neq j} l_{ij} a_{ij}$. The area covered by the mycelium was determined from the convex hull encompassing all the outermost nodes, and used to calculate the corresponding density measures for nodes, links and cost. The alpha index or coefficient (Fricker et al., 2007a; Haggett and

Chorley, 1969) provides a measure of the number of cycles present in a planar network, normalised to the maximum possible assuming there are no overlapping links:

$$\alpha = \frac{M - N + 1}{2N - 5}$$

where M is the total number of links and n the total number of nodes. Values of α range from 0 to 1 and allow comparison of networks of different sizes.

For display purposes, the image contrast was enhanced by subtracting the background signal (determined from a 2-D median filtering with a 31 × 31 pixel kernel), followed by contrast-limited adaptive histogram equalisation (CLAHE), contrast stretching and inversion of the look-up table (LUT) to give a black mycelium on a white background.

3. Results and discussion

3.1. Limited resources constrain the ability of the network to respond to grazing

P. velutina grew as a dense network (Fig. 1), with similar increases in the surface area covered by the mycelium (hyphal coverage, *HC*) in all treatments, reaching a maximum of ~550 cm^2 at 36–43 d (Fig. 2A). The untreated (R^-C^-) colonies also reached their maximum radial extent, just within the confines of the microcosm boundary (Fig. 1A), and their maximum fractal dimension, with a D_{BM} of 1.82 ± 0.01 (Fig. 2B), at about this time. Growth was initially fairly symmetrical, however, as resources in the inoculum became depleted, growth was restricted to extension of domains served by the major cords. This parallels observations made at a much earlier stage of colony development in small (12 × 12 cm) microcosms that switched from initial symmetrical diffuse growth to a limited number of growth foci coincident with the development of cords (Tlalka et al., 2008a).

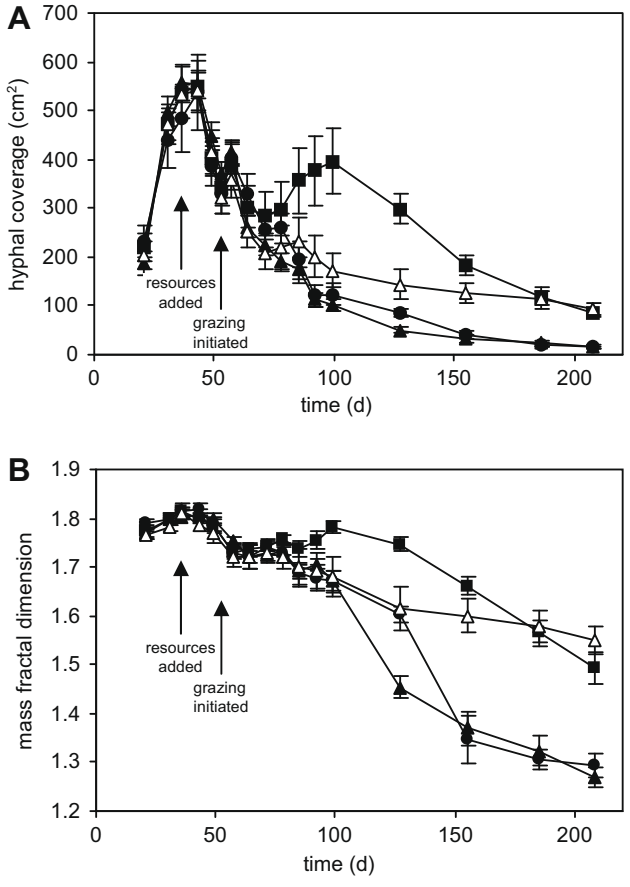

Fig. 2. Change in hyphal coverage and mass fractal dimension in response to added resources and grazing. Changes in hyphal coverage (A) and mass fractal dimension, D_{BM} (B), over time in ungrazed microcosms with no additional resources (●); grazed, no additional resources (▲); ungrazed, with additional resources (■); and grazed, with additional resources (Δ). The time of addition of extra wood resources and collembola are indicated. Values are presented as mean ± sem, $n = 7$. Repeated measures ANOVA showed a significant difference between treatments over time for both hyphal coverage ($P = 0.043$, calculated $F = 3.424$, critical $F = 3.07247$) and D_{BM} ($P = 0.036$, calculated $F = 3.561$, critical $F = 3.19678$). Data for the first 99 d are from Wood et al. (2006).

In the absence of added resources, the networks maintained a reasonable proportion of the area originally explored, but gradually thinned out the interstitial mycelium and eventually most of the major cords as well (Fig. 1A). Quantitatively, *HC* in R^-C^--microcosms dropped mono-exponentially, with a half-life of ~31 d. D_{BM} declined to a stable plateau around 1.7 that was maintained until 99 d (Fig. 2B), after which the network began to disintegrate completely. By 208 d almost all the mycelium had regressed with no sign of fresh growth (Figs. 1A and 2A). In three out of seven of the trays, the central wood block was either colonised by soil micromycetes or was completely decomposed at this stage.

In the absence of added resources, the network showed little ability to respond to the addition of collembola at 57 d (Fig. 1B). Thus, in R^-C^+-microcosms, the decline in *HC* was marginally faster ($t_{1/2} = 27$ d; Fig. 2A), and the reduction in D_{BM} was more pronounced at 127 d (Fig. 2B). There was also no evidence that such regressing networks were able to respond to grazing by the formation of additional tangential connections. By 208 d there was no mycelium remaining in 2 (of 7) microcosms, and little hyphal coverage remaining (14.5 ± 3.1 cm^2) in the other systems. Both *HC* and D_{BM} (1.26 ± 0.02) were not significantly different ($P > 0.05$) to the controls by 208 d (16.5 ± 4.8 cm^2, 1.29 ± 0.02 respectively).

3.2. Additional resources promote growth and increase cross-connectivity

The addition of four further resources (at 36 d) substantially altered the development of the networks (compare Fig. 1A and C). This did not happen immediately as it took several weeks for the new resources to become colonised before further outgrowth was observed (Fig. 2A and B). Thus, in R^+C^--microcosms (Fig. 1C), *HC* and D_{BM} both declined in a similar manner to R^-C^--microcosms until 78 d, predominantly through thinning out of the interstitial mycelium, although the rate was marginally slower ($t_{1/2} = 42$ d; Fig. 2A). Nevertheless, over this period, the network architecture did alter, with strengthening of links to the new resources and an increase in cross-connections around the blocks. After this point, there was a transient increase in *HC* (Fig. 2A), driven by both local proliferation of cords along each of the inoculum-resource axes and the emergence of new growth towards the colony margin (Fig. 1C). The interstitial growth had some similarity to transient localised patches that develop to scavenge locally for mineral nutrients in the soil which depends on the nutrient balance in the rest of the colony, and increases both if the overall mineral nutrient levels are low, and if carbon is high (Boddy et al., 1999; Wells et al., 1997). However, in the case of added resources observed here, proliferation took place over a more extensive domain within the colony, so it is less clear whether both responses are mechanistically similar.

Once mycelia re-emerged from the new resources, the amount of new growth was significantly lower than from the initial inoculum, even though there was four times the notional resource available. This might reflect the enhanced nutrient status of the mycelium in the inoculum, which had the opportunity to sequester

resources from the high nutrient media during colonisation and was thus able to forage over a much greater distance. Alternatively, the physical barrier encountered at the edge of the microcosm may have inhibited new growth. In ungrazed microcosms, fusions between advancing fronts of new growth constrained by the microcosm boundary formed circumferential connections between the newer resources. However, there was little evidence for strengthening of existing tangential paths. Some of the new interstitial cords persisted and fused to give a transient increase in tangential connectivity. However, the overall frequency of these cross-links declined as the networks regressed. From 99 d onwards, the *HC* again declined ($t_{1/2}$ = 49 d; Fig. 2A) and the network thinned out, with a decrease in D_{BM} to 1.49 ± 0.03. Given the trend over the preceeding 14 weeks, this value might be expected to decrease further over a longer period.

Connections to the central inoculum were maintained in most microcosms. Continued regression resulted in a cross-shaped morphology in many of the systems, with only major cords connecting the inoculum with each of the four new wood resources (Fig. 1C), even though the central resource was almost completely consumed. In some of the microcosms, the major cords were also observed to straighten, shorten and resolve into simpler geometric configurations (e.g. the lower arm of the cross in Fig. 3B), suggesting the cords may be subject to tension. As the cords shorten during this process, there is also the possibility that there is additional intercalary modification of cord structure, leading to more efficient overall use of resources by recycling excess material, minimising the translocation distance and reducing the tortuosity of the transport pathway.

Nevertheless, the network architecture was dominated by the legacy of the initial radial growth pattern, with relatively limited capacity to engineer new, shorter routes between added resources of higher quality until substantial new growth had occurred. Thinning out to a sparse network has some similarity to formation of shortest-path networks by *Physarum polycephalum* (Nakagaki, 2001; Nakagaki and Guy, 2008; Nakagaki et al., 2004a,b; Tero et al., 2006), or formation of foraging ant trails (Dorigo et al., 1999; Sumpter, 2006), albeit over different time scales. The slower response in mycelial networks may be a simple reflection of the different time scales required for growth and resorption of walled hyphae compared to contractile amoeboid movements. Alternatively it may provide an increased probability that the existing network will receive new inputs, before it shrinks back completely.

3.3. Grazing stimulates consolidation of the existing network and limits emergence of new growth

Grazing of the supplemented microcosms curtailed exploratory growth, and transiently reduced the *HC* as the collembola destroyed the existing network. Quantitatively, the supplemented networks responded in a similar manner to grazing as the un-supplemented microcosms (Fig. 1D), with a rapid decline in *HC* ($t_{1/2}$ = 26 d; Fig. 2A) and slower decline in D_{BM}. There was a slight, transient recovery in *HC* in R^+C^+-microcosms around 99 d, followed by a gentle decline to essentially the same level as the ungrazed R^+C^--microcosms (Fig. 2A). Nevertheless, aspects of the pattern of resource allocation were significantly different. The majority of growth occurred within the existing network as localised proliferation of fans of fine hyphae, with little sustained new growth emerging from the newly colonised wood blocks. Although, most hyphal fans disappeared rapidly, some of the fine interstitial hyphae persisted, thickened and eventually increased the level of cross-connectivity, as judged by D_{BM}, to a slightly higher level than that present in R^+C^+-microcosms (Fig. 2B). This is similar to previous observations on growing networks before resource limitation occurred (Rotheray et al., 2008). In contrast, microcosms without additional wood blocks did not appear to have sufficient resources to respond to grazing, even with resorption of the redundant mycelium.

3.4. Characterising the development of network architecture

The macroscopic properties (*HC* and D_{BM}) of the network responses to resource addition and grazing pressure were determined by the aggregated behaviour of individual cords within the network. To characterise the responses of these cords during development, changes in their thickness and connectivity were mapped for a segment of the overall network for three replicate R^+C^+- and R^+C^--microcosms and colour-coded according to the link diameter (Fig. 3A and B). Selective strengthening of the cords linking the inoculum and added resource was apparent as an increase in thickness of the intervening cords, often before there was obvious regression of the interstitial hyphae (Fig. 3A and B). The developmental evolution of each link over time was estimated from the ratio of the sum of change in thickness between each time point to the maximum change observed between 36 d and 208 d (Fig. 4). In this pseudo-colour representation, red represents continuous growth, blue continuous regression and green either no change or growth followed by regression. In R^+C^--microcosms, most growth (red) took place at the colony margin and particularly distal to the newly colonised resource (Fig. 4A–C). Nevertheless, a considerable proportion of this new growth was not sustained and subsequently declined (green). Likewise, many of the cords present at 36 d declined (blue) resolving down to a sparser network. Resource addition stimulated the formation of some new cross-links, particularly in the region between the inoculum and new resource. However, many of these subsequently disappeared (Fig. 4A). In the grazed colonies, the amount of new exploratory growth was much lower, with most of the new growth occurring within the confines of the existing network (Fig. 4B).

Quantitatively, the number of nodes (Fig. 5A) and links (Fig. 5B) per unit area in the segments of the R^+C^--microcosms showed parallel responses to the macroscopic changes in *HC* for the whole network (Fig. 2A), with a delayed, transient increase following addition of the new resources, before a substantial decline to 10–20% of the starting values by 208 d. The response in the grazed R^+C^+-microcosms was more informative. Grazing resulted in a transient drop in the node density (Fig. 5A) and link density (Fig. 5B), followed by a recovery to a level greater than that observed in the R^+C^--microcosms. Interestingly, the total volume density was comparable between the two treatments until 155 d, when the grazed colonies actually had a higher density of mycelium per unit area (Fig. 5C). It appears that the total amount of material in the grazed and ungrazed supplemented microcosms was similar over time, but was just allocated differently.

As the R^+C^--networks thinned out, the alpha coefficient increased to 0.18 ± 0.02 (Fig. 5D). The alpha coefficient is the number of complete loops within the network normalised to the possible maximum (assuming no overlapping links), to allow comparison of networks of different size. Values range between 0 and 1, and a high α index indicates a network with high levels of cross-linking. The increase seen therefore reflects an increase in connectivity of the remaining nodes, and matches the changes in D_{BM} (Fig. 2B). As the network thinned further towards the final four-armed cross configuration, the alpha coefficient dropped to 0.08 ± 0.02, equivalent to 8% of the maximum number of links that might be expected in a planar network with this number of nodes. The alpha coefficient also showed a steady decline in the grazed networks, but matched the R^+C^--networks at 155 d and 208 d (Fig. 5D).

In addition to these overall changes in cord numbers and connectivity, there were also differences in the relative cord thick-

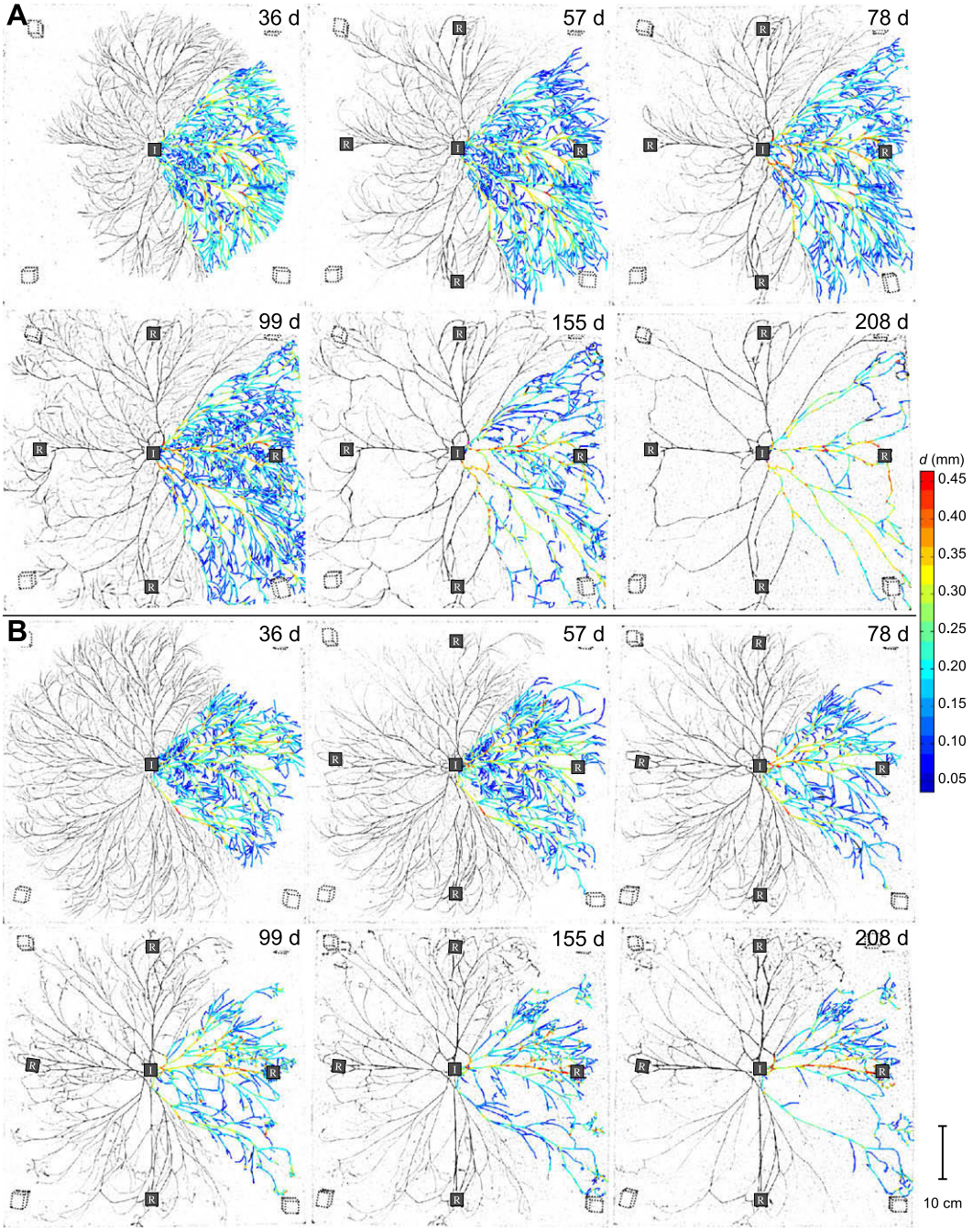

Fig. 3. Development of weighted network architecture in ungrazed and grazed microcosms. Pseudo-colour display of the evolution of link diameter for a segment of an ungrazed colony (A) and a grazed colony (B) at the time points indicated. New resources (R) were added at 36 d. The rainbow scale bar indicates relative cord thickness, red being the thickest cords. The position of Perspex lid supports are indicated by dotted outlines. I = inoculum, scale bar = 10 cm.

nesses in the ungrazed and grazed microcosms (Fig. 6A and B). Thus, for much of the developmental history of the $R^{+}C^{-}$-microcosms, there was an exponential probability distribution of cord diameter from 100 μm upwards (Fig. 6A). Nevertheless, from 155 d onwards the distribution became bimodal, with an increase in the proportion of thicker cords (Fig. 6A). This reflects the combination of continued thickening of the major cords with thinning out of the interstitial mycelium, and a decreasing population of fine hyphae as growth at the margin ceased. This transition was not observed in the grazed $R^{+}C^{+}$-microcosms, which maintained the same profile throughout the experiment (Fig. 6B).

3.5. Local cord dynamics affect predicted global network resilience

The intrinsic resilience of the network to targeted attack was assessed *in silico* at each timepoint by sequential removal of links in a sequence determined by their length and inversely by their cross-sectional area. Results were expressed as the proportion of the mass of the network that remained connected to the inoculum, against the proportion of the link area removed. In both cases values were normalised to the starting value at 36 d to accommodate absolute differences in the size of the networks (Fig. 7A and B). For the $R^{+}C^{-}$-microcosms (Fig. 7A) the connected mass, in the absence

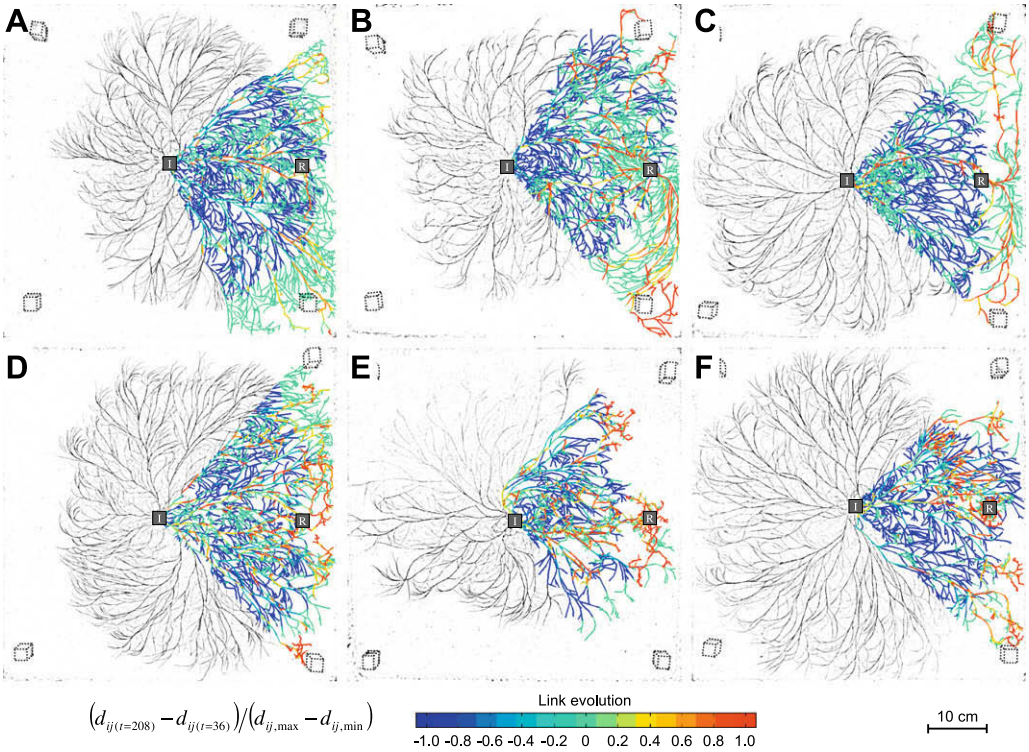

Fig. 4. Link evolution in response to grazing. Pseudo-colour display of the evolution of each link in networks with added resources (R) for three replicate ungrazed colonies (A–C) and three grazed colonies (D–F). Link evolution was calculated as the ratio between the difference in link diameter between 36 d and 208 d and the maximum difference over the whole time period. Continuous growth is indicated by red, continuous regression of cords by blue and cords that remain constant throughout are indicated by green. The pseudo-colour-coded network is superimposed on the network image at 36 d. The position of Perspex lid supports are indicated by dotted outlines. I = inoculum, scale bar = 10 cm.

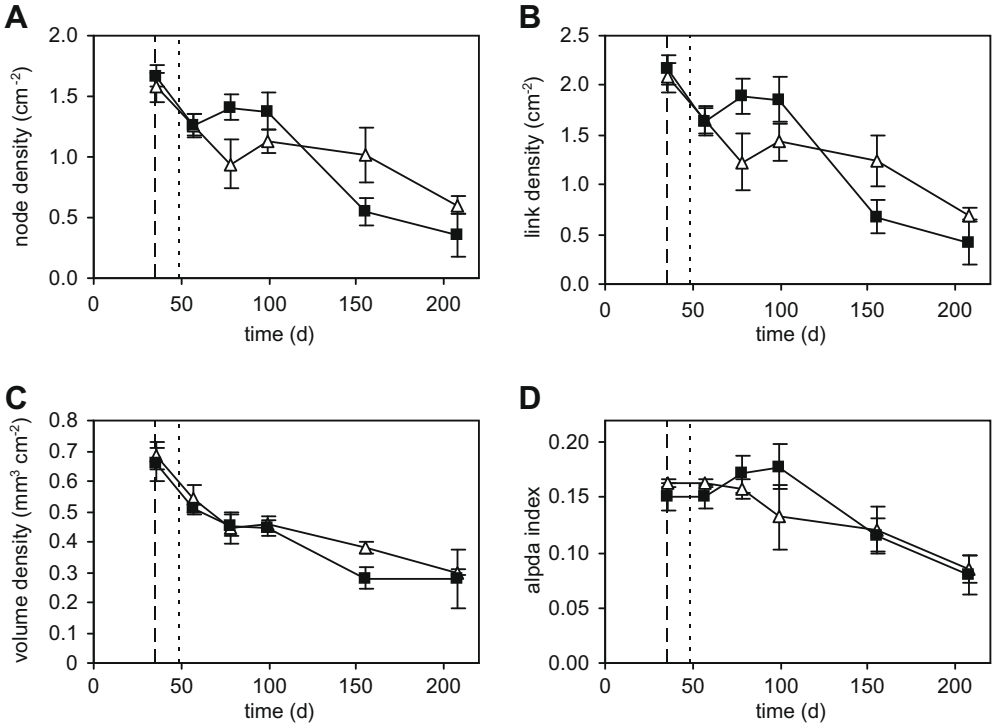

Fig. 5. Changes in network architecture in response to grazing. Characteristics of mycelial networks over time in microcosms with additional resources added at 36 d (dashed vertical line), either ungrazed (■) or grazed by collembola (Δ) added at 49 d (dotted vertical line). (A) node density given by the total number of nodes per unit area defined by the convex hull surrounding all the nodes; (B) link density; (C) cost density; (D) alpha index (coefficient). Values are presented as mean ± sem, $n = 4$ (A) or $n = 3$ (B).

of any link removal, reflected the change in *HC* (Fig. 2A). Up to 99 d, as an increasing proportion of link area was removed the connected mass declined towards a low plateau around 0.08 when 40% of the link area was severed. This corresponded to the core

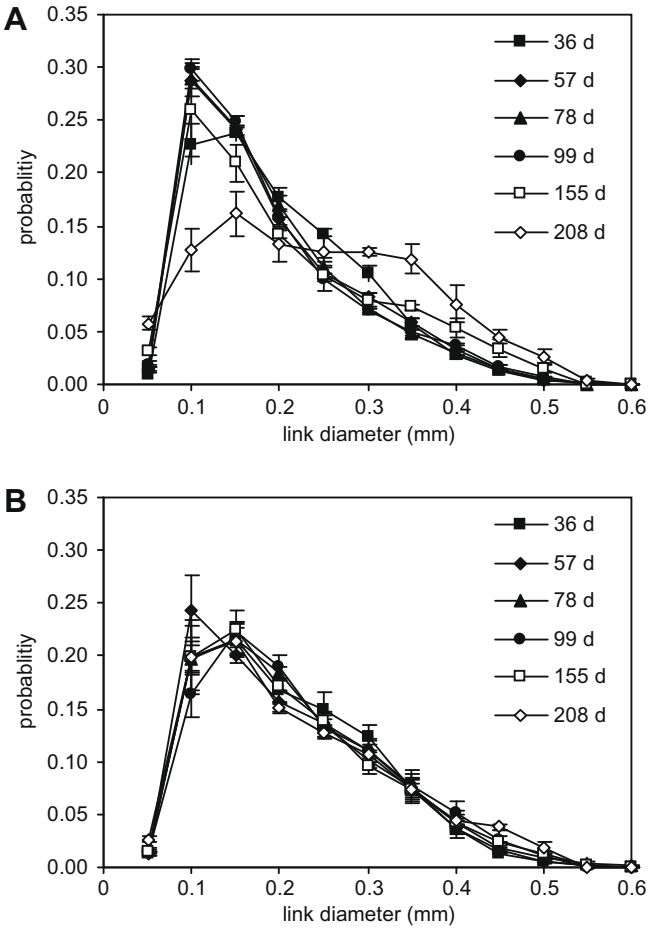

Fig. 6. Changes in the probability distributions for link diameter over time in response to grazing. The frequency of occurrence of cords with different diameters was normalised to the total number of links present at the time points indicated to examine the relative profile of links in the weighted networks in the absence (A) or presence (B) of grazing. Values are presented as mean ± sem, $n = 4$ (A) or $n = 3$ (B).

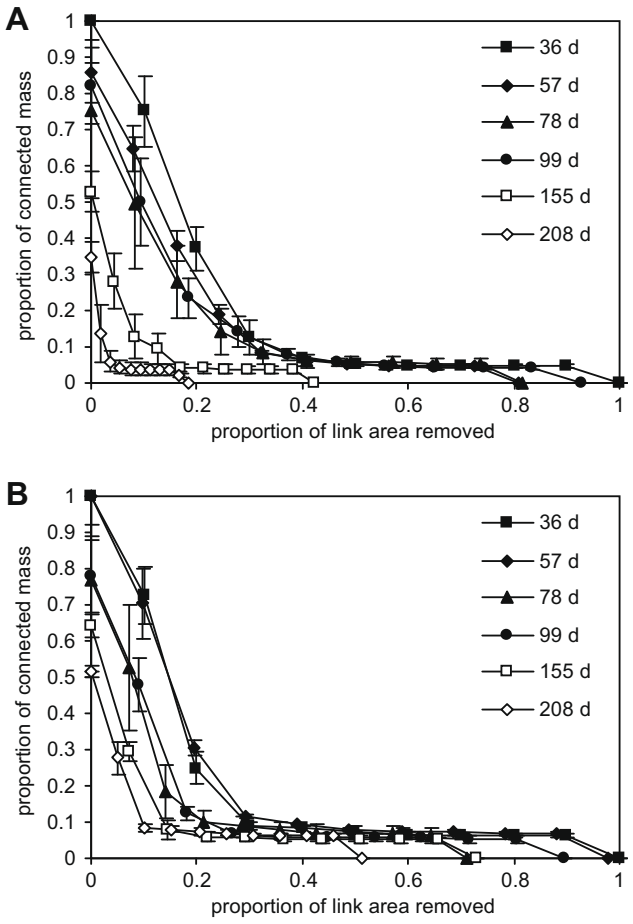

Fig. 7. Changes in predicted network resilience determined *in silico* in response to grazing. Links were sequentially removed from the weighted networks *in silico* to investigate the predicted resilience of the network at the time points indicated. Results are expressed as the proportion of the mass of the network that remained connected to the inoculum against the proportion of the link area removed in the absence (A) or presence (B) of grazing. In both cases values are normalised to the starting value at 36 d to accommodate absolute differences in the size of the networks. Values are presented as mean ± sem, $n = 4$ (A) or $n = 3$ (B).

of the thickest cords that remained between the inoculum and added resource. The networks remaining at 155 d and 208 d had considerably lower mass at the start of *in silico* link removal, and also collapsed more rapidly (Fig. 7A). Grazing altered these profiles in a complex manner. In the first 50 d after introduction of the collembola, the networks were intrinsically weaker, reaching the minimal connected core after severing of only 20% of the total link area (Fig. 7B). Importantly, however, at the later timepoints, the network proved more resilient to damage, retaining a greater connected mass and not collapsing as quickly as colonies in the R^+C^--microcosms (Fig. 7B).

Crucially, it appears that grazing initiated renewed interstitial proliferation and cross-linking at the expense of further exploratory growth, effectively re-directing resources to consolidation of the existing network. Some of the new connections were maintained and developed as new cords that increased the resilience of the network to further attack. Additional resources also stimulated increased local proliferation, but this was not developed further in the absence of grazing. We infer that the first step in response to a range of stimuli may simply require the activation of a population of relatively quiescent somatic hyphae, possibly acting in an analogous manner to stem cells in other kingdoms (Money, 2002), to produce new fine mycelium. This is then subsequently refined by retention and reinforcement of a limited sub-set of cords, probably through some form of functional feedback and recycling of redundant material through autophagy or apoptosis.

References

Albert, R., Barabasi, A.L., 2002. Statistical mechanics of complex networks. Rev. Mod. Phys. 74, 47–97.
Amaral, L.A.N., Ottino, J.M., 2004. Complex networks – augmenting the framework for the study of complex systems. Eur. Phys. J. B 38, 147–162.
Bebber, D.P., Hynes, J., Darrah, P.R., Boddy, L., Fricker, M.D., 2007a. Biological solutions to transport network design. Proc. Roy. Soc. B 274, 2307–2315.
Bebber, D.P., Tlalka, M., Hynes, J., Darrah, P.R., Ashford, A., Watkinson, S.C., Boddy, L., Fricker, M.D., 2007b. Imaging complex nutrient dynamics in mycelial networks. In: Gadd, G., Watkinson, S.C., Dyer, P. (Eds.), Fungi in the Environment. Cambridge University Press, pp. 3–21.
Boddy, L., 1993. Saprotrophic cord-forming fungi – warfare strategies and other ecological aspects. Mycol. Res. 97, 641–655.
Boddy, L., 1999. Saprotrophic cord-forming fungi: meeting the challenge of heterogeneous environments. Mycologia 91, 13–32.
Boddy, L., Donnelly, D.P., 2008. Fractal geometry and microorganisms in the environment. In: Senesi, N., Wilkinson, K. (Eds.), Fractal Structures and Processes in the Environment. IUPAC.
Boddy, L., Jones, T.H., 2007. Mycelial responses in heterogeneous environments: parallels with macroorganisms. In: Gadd, G., Watkinson, S.C., Dyer, P. (Eds.), Fungi in the Environment. Cambridge University Press, pp. 112–158.
Boddy, L., Jones, T.H., 2008. Interactions between basidiomycota and invertebrates. In: Boddy, L., Frankland, J.C., West, P. (Eds.), Ecology of Saprotrophic Basidiomycetes. Elsevier, Amsterdam, pp. 153–177.
Boddy, L., Wells, J.M., Culshaw, C., Donnelly, D.P., 1999. Fractal analysis in studies of mycelium in soil. Geoderma 88, 301–328.
Boddy, L., Hynes, J., Bebber, D.P., Fricker, M.D., 2009. Saprotrophic cord systems: dispersal mechanisms in space and time. Mycoscience 50, 9–19.
Cairney, J.W.G., 2005. Basidiomycete mycelia in forest soils: dimensions, dynamics and roles in nutrient distribution. Mycol. Res. 109, 7–20.

Donnelly, D.P., Wilkins, M.F., Boddy, L., 1995. An integrated image-analysis approach for determining biomass, radial extent and box-count fractal dimension of macroscopic mycelial systems. Binary Comput. Microbiol. 7, 19–28.

Dorigo, M., Di Caro, G., Gambardella, L.M., 1999. Ant algorithms for discrete optimization. Artif. Life 5, 137–172.

Dorogovtsev, S.N., Mendes, J.F.F., 2002. Evolution of networks. Adv. Phys. 51, 1079–1187.

Eamus, D., Thompson, W., Cairney, J.W.G., Jennings, D.H., 1985. Internal structure and hydraulic conductivity of basidiomycete translocating organs. J. Exp. Bot. 36, 1110–1116.

Fricker, M.D., Boddy, L., Bebber, D.P., 2007a. Network organisation of mycelial fungi. In: Howard, R.J., Gow, N.A.R. (Eds.), The Mycota. Springer-Verlag, Berlin, pp. 309–330.

Fricker, M.D., Tlalka, M., Bebber, D., Tagaki, S., Watkinson, S.C., Darrah, P.R., 2007b. Fourier-based spatial mapping of oscillatory phenomena in fungi. Fungal Genet. Biol. 44, 1077–1084.

Fricker, M.D., Bebber, D.P., Boddy, L., 2008a. Mycelial networks: structure and dynamics. In: Boddy, L., Franklin, J.C., van West, P. (Eds.), Ecology of Saprotrophic Basidiomycetes. Academic Press, Amsterdam, pp. 3–18.

Fricker, M.D., Lee, J.A., Bebber, D.P., Tlalka, M., Hynes, J., Darrah, P.R., Watkinson, S.C., Boddy, L., 2008b. Imaging complex nutrient dynamics in mycelial networks. J. Microsc. 231, 317–331.

Haggett, P., Chorley, R.J., 1969. Network Analysis in Geography. Arnold, London.

Karperien, A., 2003. FracLac. <http://www.geocities.com/akarpe@sbcglobal.net/usefraclac.html>.

Lamour, A., Termorshuizen, A.J., Volker, D., Jeger, M.J., 2007. Network formation by rhizomorphs of *Armillaria lutea* in natural soil: their description and ecological significance. FEMS Microbiol. Ecol. 62, 222–232.

Leake, J.R., Johnson, D., Donnelly, D.P., Muckle, G.E., Boddy, L., Read, D.J., 2004. Networks of power and influence. the role of mycorrhizal mycelium in controlling plant communities and agroecosystem functioning. Can. J. Bot. 82, 1016–1045.

Money, N.P., 2002. Mushroom stem cells. BioEssays 24, 949–952.

Moore, D., 1995. Tissue formation. In: Gow, N.A.R., Gadd, G.M. (Eds.), The Growing Fungus. Chapman and Hall, London, pp. 423–466.

Nakagaki, T., 2001. Smart behavior of true slime mold in a labyrinth. Res. Microbiol. 152, 767–770.

Nakagaki, T., Guy, R.D., 2008. Intelligent behaviors of amoeboid movement based on complex dynamics of soft matter. Soft Matter 4, 57–67.

Nakagaki, T., Kobayashi, R., Nishiura, Y., Ueda, T., 2004a. Obtaining multiple separate food sources: behavioural intelligence in the *Physarum plasmodium*. Proc. Roy. Soc. Lond. B 271, 2305–2310.

Nakagaki, T., Yamada, H., Hara, M., 2004b. Smart network solutions in an amoeboid organism. Biophys. Chem. 107, 1–5.

Newman, M.E.J., 2003. The structure and function of complex networks. SIAM Rev. 45, 167–256.

Obert, M., Pfeifer, P., Sernetz, M., 1990. Microbial-growth patterns described by fractal geometry. J. Bacteriol. 172, 1180–1185.

Petersen, H., Luxton, M., 1982. A comparative analysis of soil fauna populations and their role in decomposition processes. Oikos 39, 287–388.

R Development Core Team, 2007, A language and environment for statistical computing. R foundation for statistical computing. Vienna, Austria.

Rayner, A.D.M., 1991. The challenge of the individualistic mycelium. Mycologia 83, 48–71.

Rayner, A.D.M., Griffith, G.S., Ainsworth, A.M., 1994. Mycelial interconnectedness. In: Gow, N.A.R., Gadd, G.M. (Eds.), The Growing Fungus. Chapman and Hall, London, pp. 21–40.

Rayner, A.D.M., Watkins, Z.R., Beeching, J.R., 1999. Self-integration – an emerging concept from the fungal mycelium. In: Gow, N.A.R., Robson, G.D., Gadd, G.M. (Eds.), The Fungal Colony. Cambridge University Press, Cambridge, pp. 1–24.

Rotheray, T.D., Jones, T.H., Fricker, M.D., Boddy, L., 2008. Grazing alters network architecture during interspecific mycelial interactions. Fungal Ecol. 1, 124–132.

Rotheray, T.D., Boddy, L., Jones, T.H., 2009. Collembola foraging responses to interacting fungi. Ecol. Entomol. 34, 125–132.

Senesi, N., Boddy, L., 2002. A fractal approach for interactions between soil particles and microorganisms. In: Huang, P.M., Bollag, J.-M., Senesi, N. (Eds.), Interactions between Soil Particles and Microorganisms. Impact on the Terrestrial Ecosystem. John Wiley, Chichester, pp. 41–84.

Sumpter, D.J.T., 2006. The principles of collective animal behaviour. Phil. Trans. Roy. Soc. B 361, 5–22.

Tero, A., Kobayashi, R., Nakagaki, T., 2006. *Physarum* solver: a biologically inspired method of road-network navigation. Physica A 363, 115–119.

Thompson, W., Rayner, A.D.M., 1982. Structure and development of mycelial cord systems of *Phanerochaete laevis* in soil. Trans. Brit. Mycol. Soc. 78, 193–200.

Tlalka, M., Bebber, D.P., Darrah, P.R., Watkinson, S.C., Fricker, M.D., 2007. Emergence of self-organised oscillatory domains in fungal mycelia. Fungal Genet. Biol. 44, 1085–1095.

Tlalka, M., Bebber, D.P., Darrah, P.R., Watkinson, S.C., Fricker, M.D., 2008a. Quantifying dynamic resource allocation illuminates foraging strategy in *Phanerochaete velutina*. Fungal Genet. Biol. 45, 1111–1121.

Tlalka, M., Fricker, M., Watkinson, S., 2008b. Imaging of long-distance alpha-aminoisobutyric acid translocation dynamics during resource capture by *Serpula lacrymans*. Appl. Environ. Microbiol. 74, 2700–2708.

Watkinson, S.C., Bebber, D., Darrah, P.R., Fricker, M.D., Tlalka, M., Boddy, L., 2006. The role of wood decay fungi in the carbon and nitrogen dynamics of the forest floor. In: Gadd, G.M. (Ed.), Fungi in Biogeochemical Cycles. Cambridge University Press, Cambridge, pp. 151–181.

Wells, J.M., Donnelly, D.P., Boddy, L., 1997. Patch formation and developmental polarity in mycelial cord systems of *Phanerochaete velutina* on a nutrient-depleted soil. New Phytol. 136, 653–665.

Wood, J., Tordoff, G.M., Jones, T.H., Boddy, L., 2006. Reorganization of mycelial networks of *Phanerochaete velutina* in response to new woody resources and collembola (*Folsomia candida*) grazing. Mycol. Res. 110, 985–993.